IOP Publishing | International Atomic Energy Agency Nuclear Fusion

Nucl. Fusion **59** (2019) 112009 (16pp) https://doi.org/10.1088/1741-4326/ab0be9

Formation of hot, stable, long-lived field-reversed configuration plasmas on the C-2W device

H. Gota[1], M.W. Binderbauer[1], T. Tajima[1], S. Putvinski[1], M. Tuszewski[1], B.H. Deng[1], S.A. Dettrick[1], D.K. Gupta[1], S. Korepanov[1], R.M. Magee[1], T. Roche[1], J.A. Romero[1], A. Smirnov[1], V. Sokolov[1], Y. Song[1], L.C. Steinhauer[1], M.C. Thompson[1], E. Trask[1], A.D. Van Drie[1], X. Yang[1], P. Yushmanov[1], K. Zhai[1], I. Allfrey[1], R. Andow[1], E. Barraza[1], M. Beall[1], N.G. Bolte[1], E. Bomgardner[1], F. Ceccherini[1], A. Chirumamilla[1], R. Clary[1], T. DeHaas[1], J.D. Douglass[1], A.M. DuBois[1], A. Dunaevsky[1], D. Fallah[1], P. Feng[1], C. Finucane[1], D.P. Fulton[1], L. Galeotti[1], K. Galvin[1], E.M. Granstedt[1], M.E. Griswold[1], U. Guerrero[1], S. Gupta[1], K. Hubbard[1], I. Isakov[1], J.S. Kinley[1], A. Korepanov[1], S. Krause[1], C.K. Lau[1], H. Leinweber[1], J. Leuenberger[1], D. Lieurance[1], M. Madrid[1], D. Madura[1], T. Matsumoto[1], V. Matvienko[1], M. Meekins[1], R. Mendoza[1], R. Michel[1], Y. Mok[1], M. Morehouse[1], M. Nations[1], A. Necas[1], M. Onofri[1], D. Osin[1], A. Ottaviano[1], E. Parke[1], T.M. Schindler[1], J.H. Schroeder[1], L. Sevier[1], D. Sheftman[1], A. Sibley[1], M. Signorelli[1], R.J. Smith[1], M. Slepchenkov[1], G. Snitchler[1], J.B. Titus[1], J. Ufnal[1], T. Valentine[1], W. Waggoner[1], J.K. Walters[1], C. Weixel[1], M. Wollenberg[1], S. Ziaei[1], L. Schmitz[2], Z. Lin[3], A.A. Ivanov[4], T. Asai[5], E.A. Baltz[6], J.C. Platt[6] and the TAE Team[1]

[1] TAE Technologies, Inc., Foothill Ranch, CA, United States of America
[2] University of California at Los Angeles, Los Angeles, CA, United States of America
[3] University of California at Irvine, Irvine, CA, United States of America
[4] Budker Institute of Nuclear Physics, Novosibirsk, Russian Federation
[5] Nihon University, Tokyo, Japan
[6] Google LLC, Mountain View, CA, United States of America

E-mail: hgota@tae.com

Received 23 November 2018, revised 8 February 2019
Accepted for publication 1 March 2019
Published 5 June 2019

Abstract

TAE Technologies' research is devoted to producing high temperature, stable, long-lived field-reversed configuration (FRC) plasmas by neutral-beam injection (NBI) and edge biasing/control. The newly constructed C-2W experimental device (also called 'Norman') is the world's largest compact-toroid (CT) device, which has several key upgrades from the preceding C-2U device such as higher input power and longer pulse duration of the NBI system as well as installation of inner divertors with upgraded electrode biasing systems. Initial C-2W experiments have successfully demonstrated a robust FRC formation and its translation into the confinement vessel through the newly installed inner divertor with adequate guide magnetic field. They also produced dramatically improved initial FRC states with higher plasma temperatures ($T_e \sim 250 +$ eV; total electron and ion temperature >1.5 keV, based on pressure balance) and more trapped flux (up to ~15 mWb, based on rigid-rotor model) inside the FRC immediately after the merger of collided two CTs in the confinement section. As for effective edge control on FRC stabilization, a number of edge biasing schemes

have been tried via open field-lines, in which concentric electrodes located in both inner and outer divertors as well as end-on plasma guns are electrically biased independently. As a result of effective outer-divertor electrode biasing alone, FRC plasma is well stabilized and diamagnetism duration has reached up to ~9 ms which is equivalent to C-2U plasma duration. Magnetic field flaring/expansion in both inner and outer divertors plays an important role in creating a thermal insulation on open field-lines to reduce a loss rate of electrons, which leads to improvement of the edge and core FRC confinement properties. An experimental campaign with inner-divertor magnetic-field flaring has just commenced and early result indicates that electron temperature of the merged FRC stays relatively high and increases for a short period of time, presumably by NBI and $E \times B$ heating.

Keywords: field-reversed configuration, compact toroid, neutral beam injection, edge control, collisional merging

(Some figures may appear in colour only in the online journal)

1. Introduction

A field-reversed configuration (FRC) is a prolate, high-beta compact toroid (CT) that has closed magnetic field-lines inside the separatrix and open field-line regions of poloidal axisymmetric magnetic field with zero or small self-generated toroidal magnetic field [1, 2]. The FRC topology is generated by the plasma's own diamagnetic currents, of sufficient strength to reverse the exterior magnetic field, and the FRC only requires external solenoidal coils to hold the structure inside a confinement vessel (CV). The plasma current typically decays away in a resistive timescale but can be maintained by a current drive such as neutral beam (NB) injection (NBI). The averaged beta value of FRCs is near unity: $\langle\beta\rangle = 2\mu_0 \langle p\rangle / B_e^2 \sim 90\%$, where μ_0 is the permeability of free space, $\langle p\rangle$ is the average plasma pressure, and B_e is the external magnetic field. The edge layer outside of the FRC separatrix coalesces into axial jets beyond each end of the FRC, providing a natural divertor, which may allow extraction of energy without restriction via direct energy conversion. The FRC has potential for a fusion reactor with low-cost construction and minimal maintenance due to its simple geometry. FRCs may also allow the use of advanced, aneutronic fuels such as D-^{3}He and p-^{11}B.

In the past C-2 [3, 4] and C-2U [5, 6] FRC experiments at TAE Technologies, studying FRC behavior, as well as demonstration of the FRC plasma sustainment by NBI and edge biasing/control, were the primary goals. One of the key accomplishments in the C-2 experiments was demonstration/creation of the high-performance FRC (HPF) regime, which was set apart by dramatic improvements in confinement and stability compared to other past FRC devices [4, 7–10]. HPF plasma discharges have also demonstrated increasing plasma pressure and electron temperature T_e, indicating an accumulation of fast ions as well as plasma heating by NBI. Electrically biased end-on plasma guns and effective wall/surface conditioning inside the vacuum vessel also played important roles in producing HPF plasmas, synergistically with NBI. The HPF plasmas are macroscopically stable and microstability properties appear to be different from typical regimes in toroidal confinement devices. Ion-scale fluctuations are found to be absent or strongly suppressed in the plasma core, mainly due to the large FRC ion orbits (finite Larmor radius effect [11]), resulting in near-classical thermal ion confinement [10, 12]. In order to further improve HPF plasma parameters, the C-2U experimental program commenced after various key system upgrades from C-2, including increased total NB input power from ~4 MW (20 keV hydrogen) to ~10 + MW (15 keV hydrogen, higher current at reduced beam energy) with tilted injection angle, and enhanced edge biasing capability for boundary/stability control. The upgraded NBI and edge biasing systems enabled significant plasma performance advances and had a profound impact on C-2U performance such as: (i) rapid accumulation of fast ions (about half of the initial thermal pressure replaced by fast-ion pressure); (ii) fast-ion footprint largely determines FRC dimensions; (iii) double-humped electron density and temperature profiles (indicative of substantial fast-ion pressure) [13, 14]; (iv) FRC lifetime and global plasma stability scale strongly with NB input power; and (v) plasma performance correlates with NB pulse duration in which diamagnetism persists several milliseconds after NB termination due to accumulated fast ions. Therefore, this improved plasma state created via effective NBI is called a beam-driven FRC. Under the optimum C-2U operating conditions, plasma sustainment for ~5 + ms, as well as long-lived decaying plasma discharges of up to 10 + ms, were successfully achieved [6] and performance was mostly limited by hardware and stored energy constraints such as the NB's pulse duration and the current sourcing capability of the end-on plasma guns. Furthermore, with careful 0D global power-balance analysis [15, 16], there appeared to be a strong positive correlation between electron temperature T_e and energy confinement time; i.e. the electron energy confinement time $\tau_{E,e}$ in C-2U FRC discharges scales strongly with a positive power of T_e [6, 16], which is basically the same characteristics/trend as observed in C-2 [4]. This positive confinement scaling is very attractive, and similar features of temperature dependence have also been observed in other high-beta devices such as NSTX [17, 18] and MAST [19], whereby the energy confinement time scales nearly inversely with collisionality.

In order to further improve FRC performance as well as to overcome engineering constraints mentioned above, the C-2U device has been again upgraded to C-2W (also called 'Norman', shown in figure 1). Substantial facility changes have taken place, in which the C-2U device was completely dismantled and the brand-new experimental device C-2W was constructed within one year. The C-2W device has the following key subsystem upgrades from C-2U: (i) higher injected power (up to ~21 MW), optimum and adjustable energies (15–40 keV), and extended pulse duration (up to ~30 ms) of the NBI system; (ii) installation of inner divertors with upgraded edge-biasing electrode systems, which allow for higher biasing voltage and longer pulse operation (30 + ms), and in-vacuum fast-switching magnet coils (current up and down in a few milliseconds) inside the inner divertors that allow optimization of the magnetic field profile for effective FRC translation as well as increased thermal insulation of the peripheral plasma; (iii) increased overall stored energy in the FRC formation pulsed-power system to produce better target FRCs for effective NBI heating and current drive; (iv) fast external equilibrium/mirror-coil current ramp-up capability for plasma ramp-up and control; (v) installation of trim/saddle coils for active feedback control of the FRC plasma as well as for error field correction; and (vi) enhanced overall diagnostic suite to investigate and characterize both core FRC and open-field-line plasma performances.

The main goals of the C-2W experimental program are as follows: (i) demonstrate plasma ramp-up by NB heating and current drive; (ii) improve edge/divertor plasma performance to achieve high electron temperature both at the plasma edge and inside the core; (iii) develop plasma control on the time scale significantly longer than L/R vessel-wall time and plasma confinement times, and demonstrate controllable plasma ramp-up; and (iv) explore a wide range of plasma parameters such as plasma temperature, magnetic field and plasma size to confirm the previously emerged/obtained energy confinement scaling [6, 16]. There are also several key intermediate milestones to accomplish in scientific and engineering aspects on the C-2W experimental program in order to ensure that each subsystem of the machine operates within its designed parameters as well as to accelerate the program towards the main goals: producing robust FRC formation and translation through inner divertors; establishing adequately controlled magnetic-field structures in the inner divertor area to change it from the initial guiding straight magnetic field for FRC translation (in operations phase 1.1: OP1.1) to flared magnetic field structure (in operations phase 1.2: OP1.2), as can be seen in figures 1(*b*) and (*c*); transferring edge-biasing regions from outer to inner divertors as inner-divertor magnetic field gets flared/expanded; demonstrating first-of-the-kind active-feedback magnetic flux and plasma control on FRC experiments; demonstrating sufficient particle refueling for plasma ramp-up; demonstrating effective external magnetic field ramp-up while increasing NB energy from 15 keV to 40 keV (in operations phase 2: OP2); and, establishing effective wall conditioning in the CV and high vacuum/pumping capability in all four divertors to reduce outgassing/secondary electron emissions from vessel-wall surfaces, thus improving open-field-line plasmas. Table 1 lists key machine settings/parameters as well as functionalities in those various operating phases to briefly summarize which subsystems are required or can be used for experiments.

In the paper, the C-2W experimental apparatus and plasma diagnostic suite including newly-upgraded/developed subsystems are described in section 2. Key highlights and accomplishments of early C-2W experimental campaigns as well as characteristics of newly-obtained FRCs under different operating regimes such as in OP1.1 and OP1.2 are described in section 3, where we present a few examples of different edge-biasing schemes and its effect on FRC performance. Lastly, a summary is provided in section 4.

2. C-2W experimental device, Norman

2.1. Experimental apparatus overview

The C-2W experimental device, shown in figure 1(*a*), is the world's largest theta-pinch, CT collisional-merging system, newly built at TAE Technologies to form high flux, high temperature, stable and long-lived FRC plasmas. The C-2W device was constructed in the same place as the preceding C-2U device was located; the previous C-2U experimental program operated for about a year and then the machine was dismantled completely for C-2W. Figures 1(*b*) and (*c*) illustrate typical FRC magnetic flux lines with density contours in the C-2W device under two different operating conditions with and without magnetic field flaring in the inner divertors; these density contours are obtained from a 2D multifluid force-balanced equilibrium calculation performed with the LReqMI equilibrium code [20].

The C-2W device has ~30 m in overall length and consists of the central confinement section surrounded by two newly-installed inner divertors, two field-reversed theta-pinch (FRTP) formation sections, and two outer divertors. These seven sections can be independently isolated by large-bore vacuum gate valves. The CV is made of Inconel with an inner radius r_w ~ 0.8 m and thin wall thickness whose resistive wall time is about 2–3 ms; this allows for magnetic-field ramp up/down as required during a plasma discharge. Because of the relatively short wall time of the CV, adequately controlled external magnetic field is critical to FRC plasma confinement and plasma ramp-up. The divertor vessels are made of stainless steel and have a large internal volume (~15 m^3 each) to create high volumetric pumping during a plasma discharge; furthermore, each divertor has its own internal cryogenic pumping system with titanium gettering and LN_2 cooling to enhance its pumping capacity. The formation tubes are made of quartz, which are approximately ~3.5 m in length and ~0.6 m in diameter. The overall C-2W device accommodates an ultra-high vacuum (typical vacuum level is at around low 10^{-9} Torr range, achieved by a number of high-speed turbo pumps in the CV, divertor and formation sections) with adequately set up wall conditioning systems such as titanium (sublimation/cathodic arc) gettering and LN_2 cooling systems. Using metal gaskets for vacuum seals/boundaries also contributes to this excellent vacuum level.

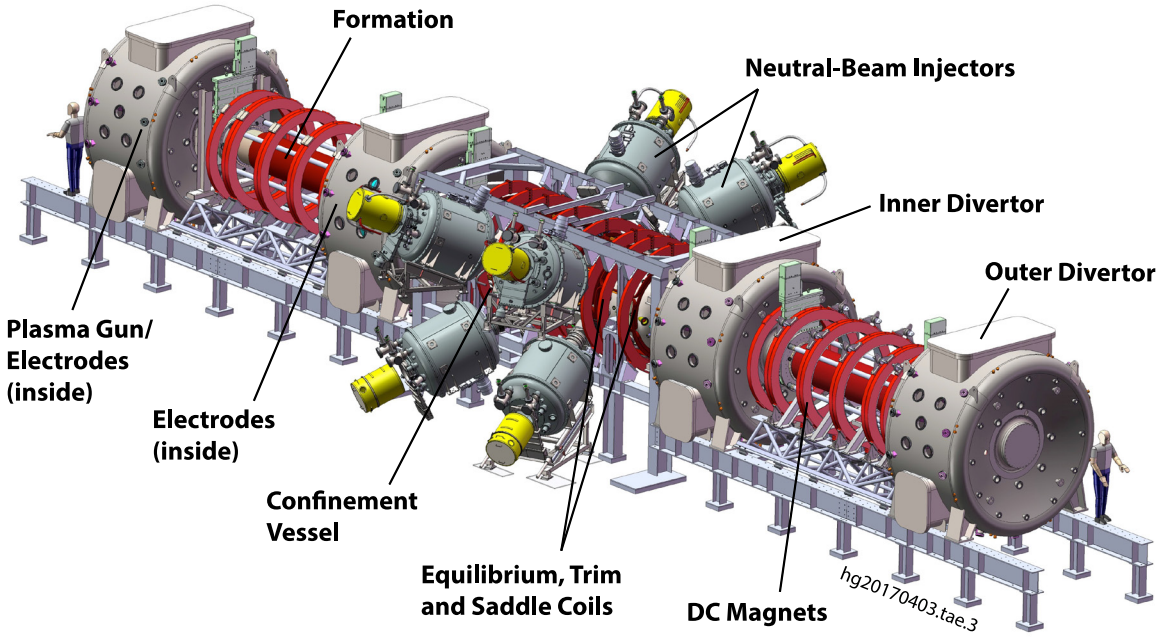

(a)

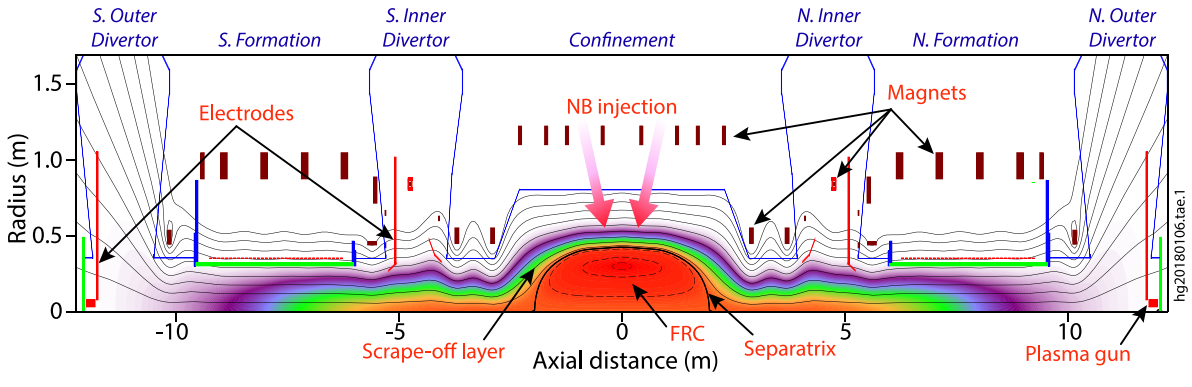

(b)

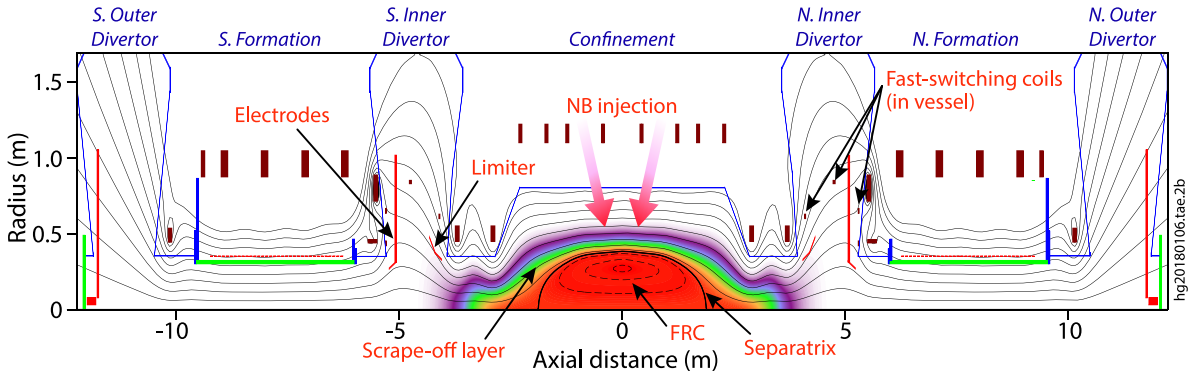

(c)

Figure 1. (*a*) Illustration of the C-2W experimental device, Norman. Sketches of FRC magnetic field-line topology and density contours in color, using 2D multifluid force-balanced equilibrium calculation performed with the LReqMI equilibrium code, in (*b*) operations phase 1.1 (OP1.1)—outer-divertor operating mode and (*c*) operations phase 1.2 (OP1.2)—inner-divertor operating mode with flared magnetic field.

There are complex magnet and control systems on C-2W that have much more operating flexibility and reliability compared to the previous C-2U device. Figure 2 shows a layout of the C-2W magnet systems, which includes the confinement equilibrium and mirror coils, saddle and trim coils, in-vacuum fast-switching coils, DC formation coils, and mirror plug coils; the coil configuration is symmetrically arranged relative to the machine midplane ($z = 0$). Note that FRTP formation coils (pulsed-power systems) are not shown in figure 2 for simplicity. A set of DC magnets and power supplies,

Table 1. C-2W machine setting and functionality in various operating phases.

	Operations phase 1		Operations phase 2
Setting/parameter	OP1.1	OP1.2	OP2
NB energy/power ramp	No (stay at 15 keV/~13 MW)	No (stay at 15 keV/~13 MW)	Yes (ramp up to 40 keV/~21 MW during a shot)
Edge biasing from outer divertor	Yes	Yes	Yes
Edge biasing from inner divertor	No	Yes	Yes
Magnetic field flaring at inner divertor	No	Yes	Yes
Equilibrium magnetic field ramp	No	No	Yes (ramp up from ~0.1 T to ~0.3 T during a shot)
Equilibrium mirror magnetic field ramp	No	Yes (optionally available)	Yes (ramp up from ~0.3 T to ~1.0 T during a shot)
Active feedback plasma control	No	Yes (optionally available)	Yes
Particle refueling	No	Yes (optionally available)	Yes

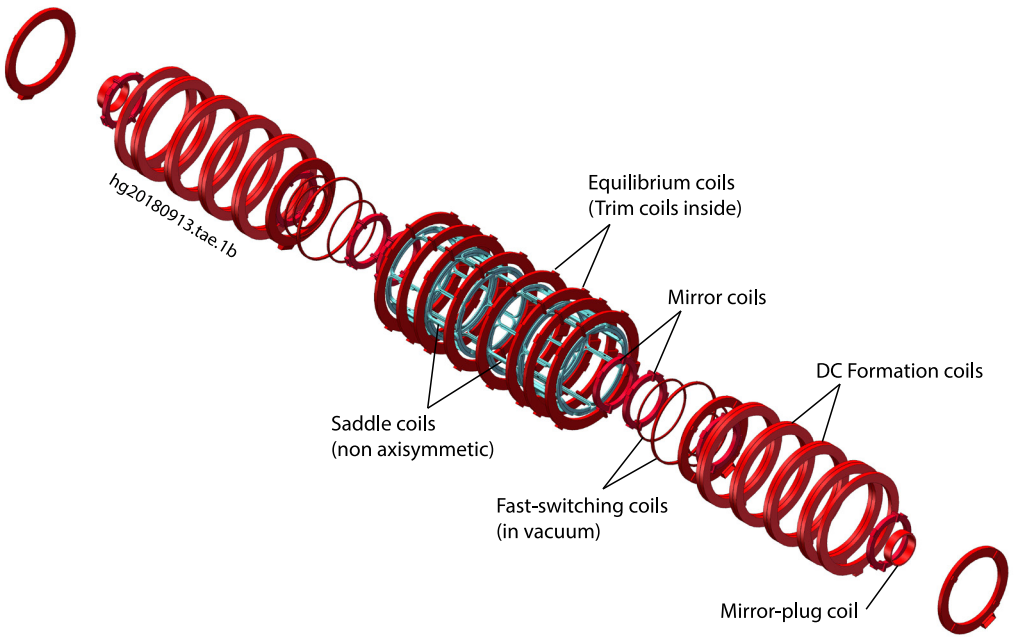

Figure 2. A layout of C-2W axisymmetric magnet systems, where non-axisymmetric Saddle coils are illustrated in cyan color. Pulsed-power formation coils/straps inside DC formation coils are not shown for simplicity.

previously used on C-2U, were repurposed on C-2W to generate a quasi-static axial magnetic field, B_z, in the formation and outer divertor regions. All other coils specified above with associated power supplies, including formation pulsed-power systems, were newly designed and developed for C-2W. Magnets and power supplies are designed to satisfy goals for the two major operating phases in the C-2W experimental program. Equilibrium magnetic fields stay constant in operations phase 1 and are ramped up during a shot in phase 2, as listed in table 1; the typical magnetic fields in those phases are B_z ~ 0.1 T increasing to ~0.3 T, respectively, while the mirror ratio of the magnetic fields in the confinement section is maintained at about 3.0–3.5 even during the field ramp and at the flat-top. Current waveforms of each equilibrium and mirror coils are independently controlled, which allows for an adequate and flexible control of the external magnetic field profile as well as plasma shape and position. Trim coils are placed beneath each of the equilibrium coils, as shown in figure 2, that can operate independently to correct error fields as well as to perform active feedback control. Non-axisymmetric saddle coils are deployed around the CV that can be operated either passively with a shorted-coil configuration or actively with power supplies for plasma position control. There are a set of in-vacuum fast-switching coils inside the inner divertors in order to provide adequate guide magnetic fields during FRC translation and then to quickly flare the fields (by reversing coil current within a few milliseconds), as depicted in figures 1(*b*) and (*c*). Magnetic mirror plugs are placed in between the formation and outer divertor sections at each side of the device that can produce a strong magnetic field up to ~1 T. The mirror-plug coils as well as confinement mirror coils play an important role in contributing to the open-field-line plasma confinement as previously reported [8, 10] and also studied in mirror devices such as GDT [21, 22].

Initial FRC plasma is generated by newly upgraded pulsed-power systems in the formation section that is basically the

same dynamic FRTP formation technique utilized in C-2 [3]. The formation pulsed-power systems consist of Bias modules for negative-bias magnetic field, main-reversal (MR) modules for main theta-pinch magnetic field, and rotating magnetic field modules for deuterium gas pre-ionization in the formation section. The previously used ringing pre-ionization (PI) system is no longer used in C-2W; the load sharing between the PI and MR capacitor banks led to mis-firing/discharging issues which limited stored energy and reliability. Note that we define '$t = 0$' in our FRC experiment as the time when the first MR module gets discharged/triggered. Each pulsed-power module has substantial system upgrades from the previous C-2/2U pulsed-power systems; the stored energy of each system has increased significantly, triggering efficiency has increased, and the overall system reliability and operating performance has improved considerably. Due to such improved overall pulsed-power system performance, the generated initial FRC plasma in the formation section has more magnetic and kinetic energies which enables a path to higher thermal energy in the CT collisional-merging process as observed in C-2/2U [3, 23].

To control open field-line plasmas as well as to provide sufficient radial electric field for $E \times B$ shear flow around the FRC separatrix, coaxial plasma guns and concentric annular electrodes are installed inside of each outer divertor as illustrated in figure 1(*b*). This edge-biasing/control configuration with a capability of magnetic field flaring at end divertors is essentially the same as C-2U [5, 6], but the C-2W edge-biasing system has more functionality and flexibility in terms of its operations such as higher voltage/potential that can be applied on the electrodes with longer pulse duration up to ~30 ms. Furthermore, similarly designed/developed annular electrodes (with a large hole in the central electrode, required for FRC translation) as well as funnel limiters are installed inside inner divertors as shown in figure 1(*c*). Electrical potentials on those inner-divertor electrodes/limiters as well as on outer-divertor electrodes can be controlled independently by power supplies. Control of magnetic field topology and boundary potentials in the divertors is the key to flexible C-2W experiments, enabling effective edge/boundary control of FRCs via open field-lines/scrape-off layer (SOL). The role of the SOL and divertors is not only to provide a favorable boundary condition for the core FRC plasma but also to handle energy and particle exhaust from the core. There is also a halo region, outside of the SOL, with open field-lines contacting to the limiters and wall of the CV that produces secondary electron emission/wall recycling; the region contains low temperature, low density partially ionized plasma sustained by power flow from the plasma core, beam ions, and warm neutrals. Therefore, adequate wall conditioning with sufficient pumping capability is important and required in order to effectively inject NBs into FRC with small charge-exchange losses.

Eight newly upgraded NB injectors are installed on the CV as shown in figure 1(*a*) for plasma heating, current drive, and partial particle refueling. The C-2W NBI system has the following key features: NB's input power and pulse duration increased from ~10 MW (15 keV hydrogen, co-current injection)/~8 ms in C-2U to 13 + MW (fixed energy of 15 keV hydrogen)/up to ~30 ms in C-2W phase 1 operations that is being further increased up to ~21 MW with tunable beam energy of 15–40 keV (four out of eight NBs will eventually have tunable energy capability) in phase 2 operations; tilted NBI angle in a range of 65°–75° (presently fixed at 70°) relative to the machine axis with average NBI impact parameter at ~19 cm to enable sufficient coupling between the beams and the target FRC plasma. The NBs provide energetic particles with a large orbit size crossing inside and outside of the FRC separatrix that stabilize global magnetohydrodynamic (MHD) modes; they also provide a significant amount of fast ion population and pressure inside the core, thus producing an advanced beam-driven FRC plasma. Ramping up CV fields in phase 2 operations will be matched by increased beam energy so as to match orbits; additionally, charge-exchange losses will be reduced at the higher particle energy, total NBI power will increase, and the fast-ion and plasma pressure will increase as well.

Plasma particle inventory must be controlled to maintain proper densities for NB capture, which is required in the presence of particle losses from the core that is unavoidable. A plasma refueling system must be capable of matching the particle losses as well as increasing the total particle inventory if desired. Diamagnetic current within the FRC flows across magnetic field lines and thus sustainment of total pressure gradient in the core is essential for sustainment of trapped flux and FRC magnetic configuration. Without central refueling or heating the trapped magnetic flux decays due to finite plasma resistivity across the magnetic field. To that end, there are three main particle refueling systems deployed on C-2W: multi-pulsed CT injector systems near the CV midplane [24, 25], a cryogenic pellet injector system [26], and gas puffing systems at both ends of the CV (near confinement mirror regions) as well as near mirror-plug regions for open-field-line plasmas. Contrary to the cryogenic pellet injection (over dense and cold gas), CT-injection refueling system can supply hotter plasma particles with controllable density level, resulting in less plasma cooling [25]. Gas puffing in the CV cannot provide effective core refueling but can be used for the edge density control.

2.2. Plasma diagnostic suite

The C-2W device is planned eventually to have more than 50 plasma diagnostic systems installed on the CV, inner/outer divertors, and formation sections. The role of the plasma diagnostic suite is to investigate and characterize not only core FRC plasma performance but also open field-line plasmas at various areas such as SOL/Jet regions and inside divertors. Figure 3 illustrates a schematic view of C-2W showing four distinct zones (core, SOL/Jet, divertors, and formation) of diagnostic interest with abridged lists of diagnostics deployed in each zone. To support C-2W experiments towards the program goals, the diagnostic suite has been significantly upgraded from the previous diagnostic suite in C-2U [27]. Much of the expansion and improvements were driven by a highly increased interest in the open-field-line plasma, which has a large impact on the core FRC and overall system performance. Furthermore, some key plasma parameters (e.g. temperatures, density/pressure, and magnetic flux) are expected to evolve in time as external magnetic field and NB input power are

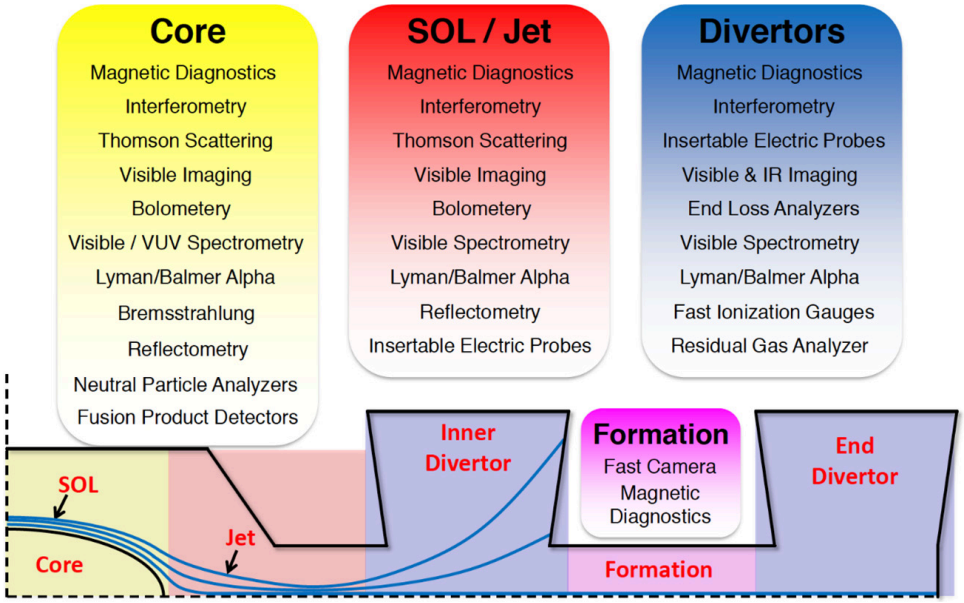

Figure 3. Schematic of C-2W showing four distinct zones/regions of diagnostics interest such as Core, SOL/Jet, divertors, and formation with abridged list of instruments.

ramped up. Consequently, broad operating range and functionality for each diagnostic system is essential on C-2W. As shown in figure 3, plasma performance and parameters at different zones/areas are investigated and provided by a comprehensive suite of diagnostics that includes magnetic sensors [28], Langmuir probes [29], far-infrared interferometry/polarimetry [30], Thomson scattering [31], VUV/visible/IR spectroscopy, bolometry, reflectometry [32], energy analyzers [33], neutral particle analyzers, fusion product detectors, secondary electron emission detectors [34], and multiple fast imaging cameras [35]. In addition, extensive ongoing work focuses on advanced methods of measuring separatrix shape and plasma current profile that will facilitate equilibrium reconstruction and active control of FRCs [36]. More detailed information of the C-2W diagnostic suite can be found elsewhere [37]. Signals and data from individual diagnostics are transferred to a data-acquisition system that acquires about 2500 channels on every C-2W discharge currently and will increase as new diagnostics, measurements, and other subsystems come online. The acquired raw data is post-processed into plasma parameters and then stored on a physics database for further data analysis. Some raw data, such as magnetic probe signals, get processed continuously during a plasma discharge through the real time control system for use in active feedback control of the plasma. On typical C-2W discharges ~4 gigabytes of data are currently generated after each shot, including analysis movies and computations; this data size will also increase as more signals with longer timescale get acquired and post processed for physics parameters.

3. C-2W experiments and results—operation phase 1

C-2W/Norman is a brand-new experimental device with substantially upgraded subsystems compared to C-2U, as described in the previous sections. Early C-2W experimental program efforts have been mostly devoted to subsystem commissioning/conditioning as well as to exploration of new operating parameters/settings, particularly in the formation pulsed-power systems and magnetic field profiles/waveforms in the CV and divertor areas. In order to gain early assurance of system functionality and develop robust FRC formation and translation schemes, C-2W experiments commenced with a single-sided configuration where half of the device was initially constructed and operated while the other half was still being built. In C-2W operation phase 1, as listed in table 1, there are two major operating configurations/conditions: operations phase 1.1 (OP1.1)—keeping strong guiding magnetic field at inner-divertor regions (in other words, without magnetic field flaring) so that C-2W can operate in a 'C-2/2U like' machine configuration; operations phase 1.2 (OP1.2)—flaring magnetic field at inner-divertor regions with transferring edge biasing/control areas from outer to inner divertors. In a simple picture, this basically changes the operating machine configuration from figures 1(*b*) and (*c*). This section describes (i) key physics/engineering elements to produce an advanced beam-driven FRC plasma on C-2W, (ii) early experimental results using single-sided machine configuration to ensure and validate a robust FRC formation as well as its translation through the inner divertor, and (iii) newly obtained experimental results with a full C-2W machine configuration in operation phase 1—with/without flaring magnetic field at inner-divertor regions but no field ramp-up or NB input power increase, as shown in table 1.

3.1. Advanced beam-driven FRCs

As previously identified and discussed in C-2/2U experiments [4, 6, 7], producing a well stabilized initial target FRC for effective NBI is the important key to achieve/obtain a

beam-driven FRC plasma state since it typically takes ~1 ms for the injected fast ions to accumulate and develop sufficient pressure inside the FRC. An HPF equilibrium state was first obtained in the C-2 device, and then further improved/advanced in C-2U to a beam-driven FRC plasma state via increased injection power of NBs and effective edge biasing/control in which FRC plasma was successfully maintained for 5 + ms. To achieve both HPF and beam-driven FRC operating conditions in C-2/2U, the following key elements/approaches were identified as necessary: (i) dynamically colliding and merging two oppositely-directed CTs for a robust FRC formation; (ii) effective wall conditioning inside vacuum vessels, e.g. using a titanium gettering system, for background neutral and impurity reduction; (iii) effective edge/boundary control around the FRC separatrix via end-on plasma guns and concentric annular electrodes inside end divertors; and (iv) effective NBI into FRCs for current drive and heating. The main feature/characteristics of those high-performance beam-driven FRC regimes are: macroscopically stable plasma discharges, dramatically reduced transport rates (up to an order of magnitude lower than the non-high-performance FRC regime), high fast-ion population/pressure inside the FRC, long-lived plasma/diamagnetism lifetimes, and emerging global energy confinement scaling with strongly favorable temperature dependence.

The key elements specified above for C-2/2U experiments are still important and critical to the C-2W experimental program. In order to enhance fast-ion effects by NBI as well as to further improve FRC performance towards the program goals, those key elements (i)–(iv) have been significantly upgraded in C-2W as described in section 2. Furthermore, two more key elements were added in C-2W: (v) adequate particle refueling into FRC core and edge for plasma density and particle control, and (vi) actively controllable external magnetic field for plasma shape/position control. These additional elements are critical, particularly in operations phase 2, for the expected FRC plasma ramp-up with increased NB input power of up to ~21 MW. Under no plasma ramp-up experimental conditions in C-2W, such as in operations phase 1, the key elements to produce a decent (stable, long lived, and hot) FRC plasma state/condition are fundamentally the same as in C-2/2U experiments even with C-2W's slightly different machine configuration (e.g. presence of inner divertors, larger diameter of the CV). However, significantly upgraded NBs and edge biasing/control systems, as well as extensive FRC/system optimization processes, have led to further improved FRC performance, ultimately showcasing an 'advanced beam-driven FRC' equilibrium state in C-2W.

3.2. Robust initial FRC formation and translation

FRCs are produced/formed by colliding and merging two oppositely-directed CTs using the FRTP method in the formation sections. This flexible, well controllable dynamic FRC formation technique [3] allows formation of various initial target FRC states for effective NBI study and plasma performance optimization. This formation technique was well-established initially on C-2, and also used in C-2U without a major upgrade in the pulsed-power systems. In C-2W the formation pulsed-power system is significantly upgraded to form more robust FRCs as well as better targets for NBI. Another important change from C-2/2U to C-2W is the new large divertor placed between the formation section and the CV as illustrated in figure 1. This requires that FRCs generated in the formation section must be robust enough to translate through the inner divertor area (~1 m gap without a conducting wall/shell) without too much degradation.

To test and verify an appropriate FRC formation and translation with the inner-divertor vessel, the C-2W experimental program commenced early as part of subsystem commissioning using only one side of the device. One side of the formation pulsed-power system, inner-divertor fast-switching coils, mirror-plug coil, and confinement equilibrium/mirror coils were thoroughly tested for functionality as well as to characterize/optimize FRC formation and translation during this early phase of experiments. Relatively good FRC plasmas were formed in the formation section and then successfully translated through the inner divertor with adequate guide magnetic field applied by the in-vacuum fast-switching coils and confinement mirror coils in the single-sided machine configuration. In this early experiment, the translated FRC plasmas had an axial speed of 150–200 km s^{-1} entering into the CV, even with slightly reduced formation pulsed-power voltages, and reached all the way to the other end of the CV where they reflected off the strong confinement-mirror magnetic field. After some dedicated tuning/conditioning of the formation pulsed-power systems with higher voltages on the MR modules, axial speed of the translated FRC got increased significantly, roughly twice as fast (sometimes up to ~500 km s^{-1}); an example of successful FRC translation entering the CV is shown in figure 4 where the diamagnetic signal contour indicates that FRC enters the CV at around 20 μs, bounced back-and-forth by the strong confinement-mirror fields at both ends of the CV, and finally settling down near the midplane ($z = 0$). This successful experimental test of the FRC formation and translation was also simulated and verified using the Lamy Ridge 2D resistive MHD code [38] using the actual experimental machine settings as its input parameters, at which the simulation result shows a consistent picture of the FRC formation/translation process as observed in the C-2W single-sided experiment; note that an example of good agreement between experiment and Lamy Ridge simulation can be seen in figures 2 and 4 of [23] for C-2 experiment. Figure 5 shows an example of the single-sided FRC simulation on C-2W, depicting a time sequence of the simulated FRC plasma (field lines and density contour) at three phases of the formation, translation through inner divertor, and near the end of translation in the CV. During this FRC formation/translation study in both experiment and simulation, it was clearly observed and verified that having an adequate guide magnetic field (using in-vacuum fast-switching coils) inside inner divertor is critical for FRC translation. Additionally, a proper balance of magnetic field amplitudes and axial profile generated by the fast-switching coils and confinement mirror coils was found to be necessary; otherwise, FRCs do not properly penetrate through the inner divertor and mirror region and can either reflect off

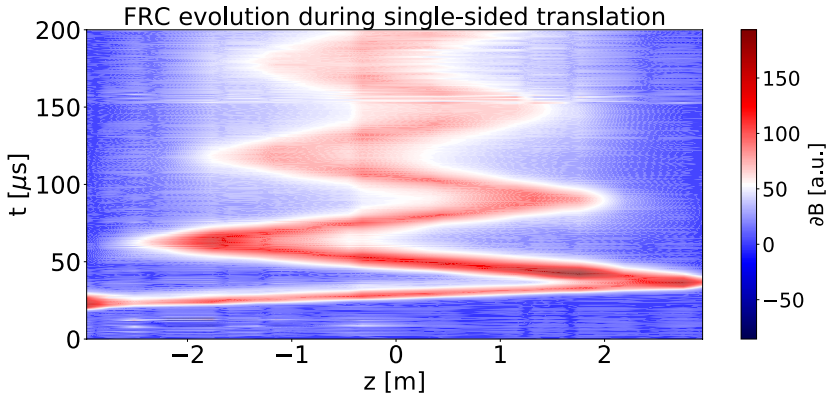

Figure 4. Example of single-sided FRC translation: time sequence of the translated FRC's diamagnetism (∂B) in the CV, where FRC is entering the CV at around 20 μs and bounced back-and-forth between mirror regions.

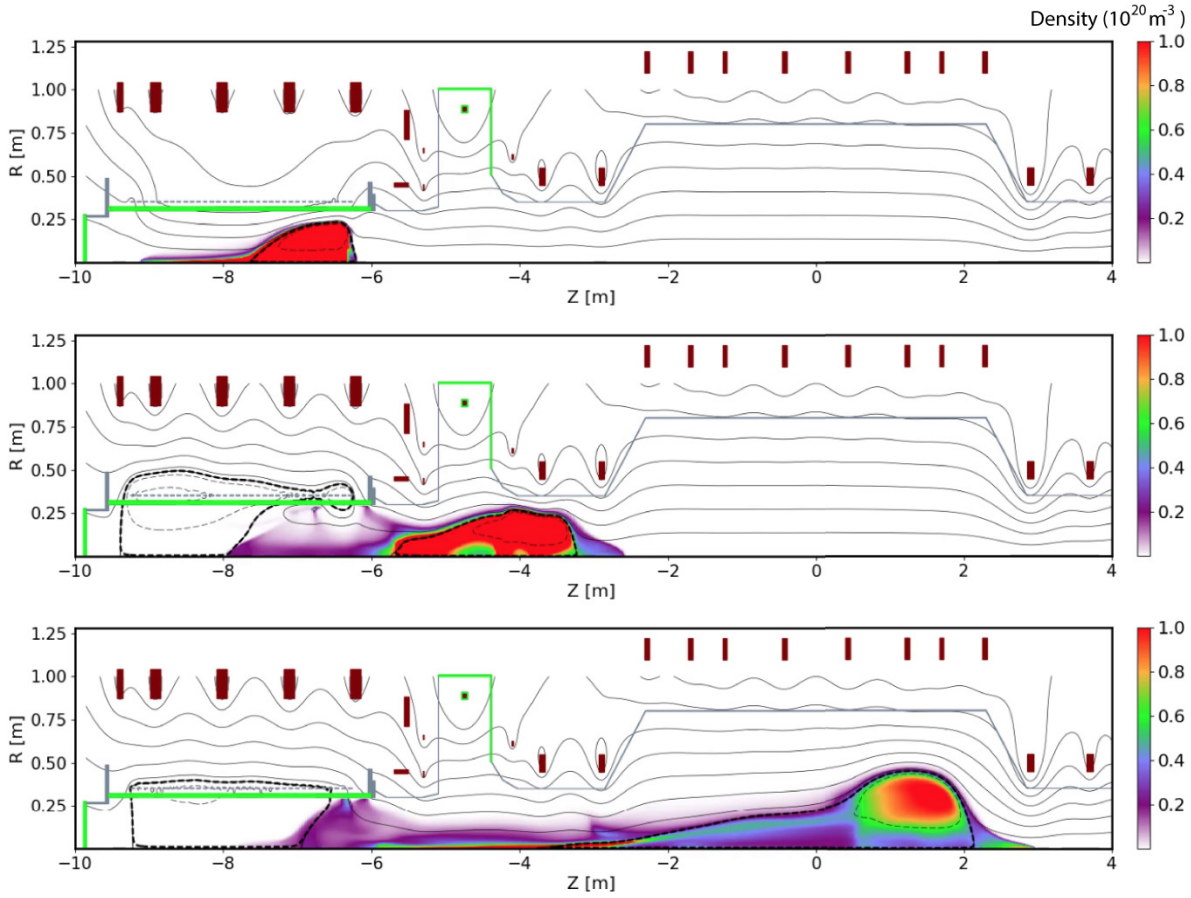

Figure 5. Two-dimensional resistive MHD simulation of FRC formation and translation in the single-sided C-2W configuration/setup, showing evolution of magnetic field lines and density contours in color at FRC formation (top), translating through inner divertor and entering the CV (middle), and fully travelled to the other end of CV (bottom).

the mirror field and become trapped inside the inner divertor, or be torn apart with partial translation into the CV [39].

3.3. Key initial results of collided/merged FRC plasmas (in operation phase 1)

C-2W experimental program has continued after completing a majority of the machine construction that includes double-sided FRC formation sections, outer-divertor edge-biasing systems, NBI system, and other key subsystems. As described earlier, our intent/objective in this operation phase 1 is to produce a decent, stable FRC target primarily for effective NBI before ramping up internal plasma pressure by increasing/ramping NB input power (planned in operations phase 2). Double-sided FRC formation, translation, and collisional merging process in C-2W is essentially the same as previous C-2/2U experiments, with the new complication of translating through the inner divertor. As described in section 3.2, initial FRC plasma formation and translation through the inner divertor is no longer the issue/concern but finding

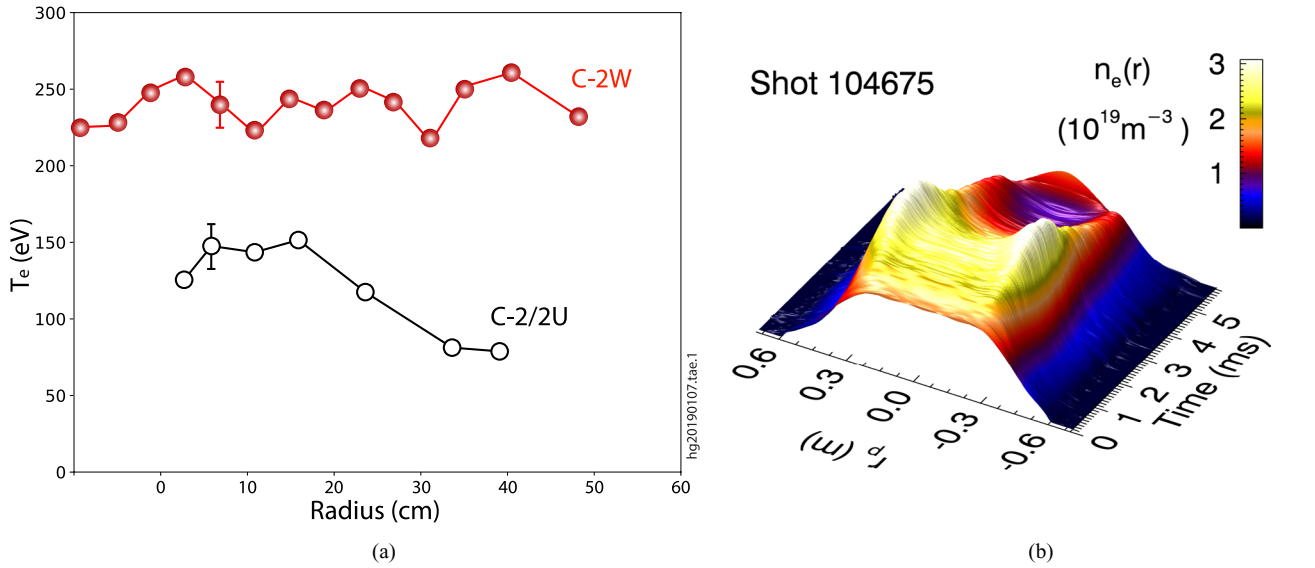

Figure 6. (*a*) Shot-averaged electron temperature profiles from midplane Thomson scattering system measured during FRC collisional merging ($t \sim 0.05$ ms), compared with a typical shot-averaged C-2/2U T_e result; typical error bars for each case are also included. (*b*) Time evolution of electron density radial profile from midplane FIR interferometer on C-2W.

and optimizing the best outcome/product after the FRC collisional-merging process remains to be obtained. We have spent a considerable amount of time to map out new operating regimes in many subsystems as well as to optimize FRC performance inside the CV. The early experimental campaign was conducted without flaring magnetic field at inner-divertor regions to obtain C-2U like long-lived stable FRC plasmas with similar machine configuration to C-2U. In this early phase of machine/plasma multi-dimensional parameter mapping, the optimization tool/algorithm previously developed with Google [40] was effectively used to find optimum operating regimes and accelerated our experimental program and progress considerably.

Remarkably improved initial FRC formation and plasma states on C-2W have the following characteristics: forming and translating more energetic FRCs (CT plasmoids), much faster translation velocity (relative speed of the two-colliding FRCs gets up to ~1000 km s^{-1}), and very flexible and wide range of operating parameters due to the upgraded pulsed-power and magnet systems. The high initial translational kinetic energy of the colliding FRCs yields high thermal energy post merging via shock heating (predominantly in the ion channel), as seen in C-2/2U [3, 23]; reconnection heating during the FRC-merging process may also contribute to the observed thermal energy increase, as seen and described in other CT-merging experiments [41, 42]. As anticipated by design and also in our simulations, the merged initial FRC state exhibits much higher plasma temperatures (in both electrons and ions), larger volume, and more trapped flux as compared to C-2U, providing a very attractive target for effective NBI in C-2W. The typical FRC plasma state right after the collisional-merging process has the following plasma properties: excluded-flux radius $r_{\Delta\phi} \sim 0.45$–0.5 m, length $l_s \sim 2.5$–3.0 m, rigid-rotor poloidal flux $\phi_p \sim 10$–12 mWb, electron temperature $T_e \sim 200$–300 eV, total temperature ($T_{tot} = T_i + T_e$, estimation based on pressure balance using density and magnetic measurements [1]) up to ~1.5–2.0 keV, and electron density $n_e \sim 1.5$–3.0×10^{19} m^{-3}. Figure 6(*a*) shows initial T_e profiles, measured by multipoint Thomson scattering system during FRC collision/merging ($t \sim 0.05$ ms) in a typical shot-averaged C-2W discharge as compared to C-2/2U experiments. The initial ~250 eV flat T_e profile (T_{tot} exceeding 1.5 keV) in C-2W is testament to the improved initial FRC conditions produced by the upgraded formation pulsed-power systems. Time evolution of the Abel-inverted n_e profile measured by 14-chord FIR interferometry is shown in figure 6(*b*) and clearly exhibits the expected hollowness of the radial density profile, corroborating a typical FRC structure. Plasma behavior inside the CV is also visually monitored by side-on fast-framing camera as illustrated in figure 7(*a*), which has a wide field of view to see FRC plasma almost entirely. One example image (with a bandpass optical filter of oxygen 4 + line) of typical plasma discharge at $t \sim 1$ ms is shown in figure 7(*b*). A football-shaped plasma emission in the CV is clearly seen, and the edge of the emission (boundary of hot/cold plasmas) is consistent with the FRC shape/profile as estimated from the excluded-flux radius measurements, depicted with dashed lines in the camera image. Using this fast-framing camera, together with FIR interferometer and Mirnov probes, global MHD instabilities such as $n = 1$ wobble/shift and $n = 2$ elliptical/rotational modes are well diagnosed in C-2W.

In order to effectively inject fast ions into the FRC plasmas without causing too much charge-exchange losses due to background neutrals, titanium gettering systems are deployed inside the CV and in all four divertors for further impurity reduction and additional vacuum pumping capability. Reducing background neutrals outside of the FRC is one of the key elements to improve NB-to-FRC coupling and its efficiency. The gettering system inside the CV currently covers more than 80% of the total surface area of the CV inner wall, and has significantly reduced the neutral recycling at the wall and greatly reduced impurity content (e.g. oxygen, carbon,

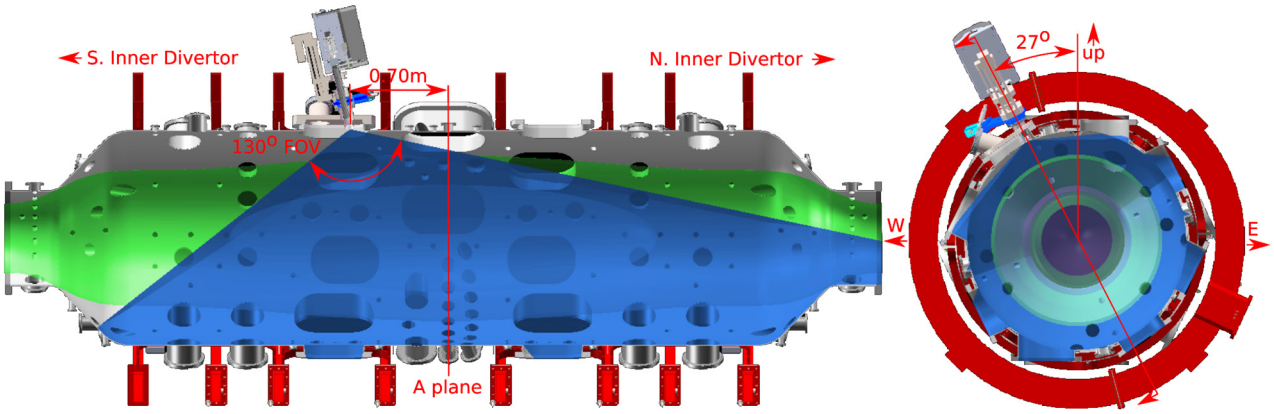

(a)

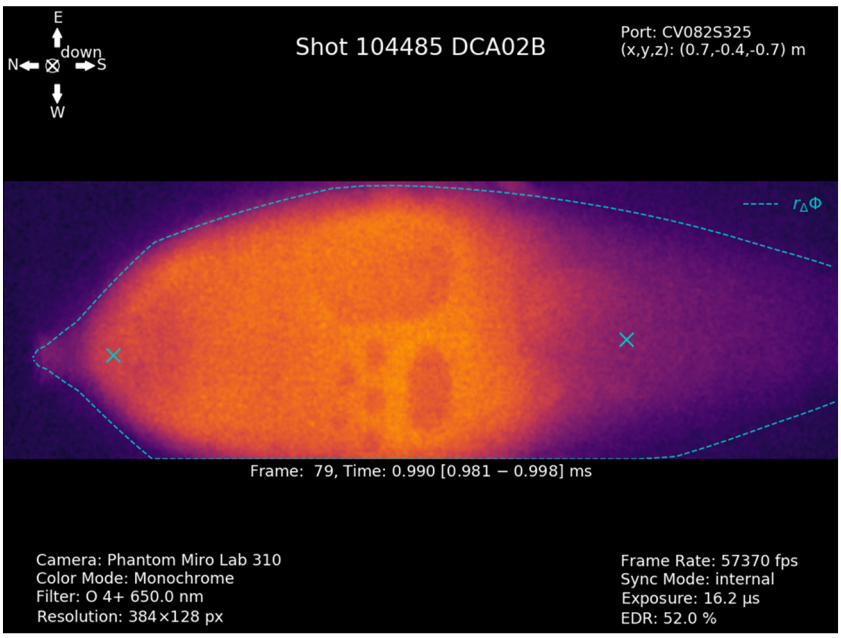

(b)

Figure 7. (*a*) Illustration of the C-2W CV with fast-framing camera setup and its field of view from near the top of the CV. (*b*) Camera image of FRC plasma emission with O 4+ bandpass optical filter ($\lambda \sim 650.0 \pm 0.5$ nm) at $t \sim 1$ ms in a typical plasma discharge; fitted excluded-flux radius profile measured by magnetic probes is also overlaid (dashed lines) in the image.

and nitrogen). Newly installed cryo-panels and a titanium arc gettering system with a liquid N_2 cooling system inside all four divertors are working effectively as designed; divertor pumping tests indicate that system pump speed has achieved up to ~2000 $m^3\ s^{-1}$ (for hydrogen) per each divertor. The titanium-arc gettering system can also be operated in between plasma shots/discharges as desired to improve/recover the divertor pumping capability. Overall FRC plasma performance, in particular lifetime and temperatures, has considerably advanced with improving wall conditioning by extensive titanium gettering in the CV and divertors [43].

As for edge biasing and boundary control of the FRC and open-field-line plasmas, there are several techniques implemented in the C-2W divertor areas as described in section 2.1: applying negative or positive voltages on the plasma guns, outer-divertor electrodes, inner-divertor electrodes, and/or funnel limiters relative to the machine ground or even to other biasing systems/points. There are so many different biasing options/configurations using those systems, that finding and mastering the most effective biasing schemes for plasma edge control is currently one of the most important objectives to achieve in this operations phase 1. Here, we present two examples of different schemes and effects to illustrate the challenges of balancing different effects on FRC performance against each other. As the first example of edge biasing scheme, as routinely used in C-2/2U experiments and well described in [7], applying negative radial electric field ($-E_r$) in the open field-lines around the FRC separatrix produces $E \times B$ shear flow that counters a natural FRC rotation in the ion diamagnetic direction, thus $n = 2$ rotational mode can be effectively stabilized in C-2W. Figure 8 shows an example of the effect of edge biasing on FRC stabilization using $-E_r$ applied edge-biasing systems in outer divertors, where the central electrode was charged up at around -1.5 kV right after $t = 0$. In

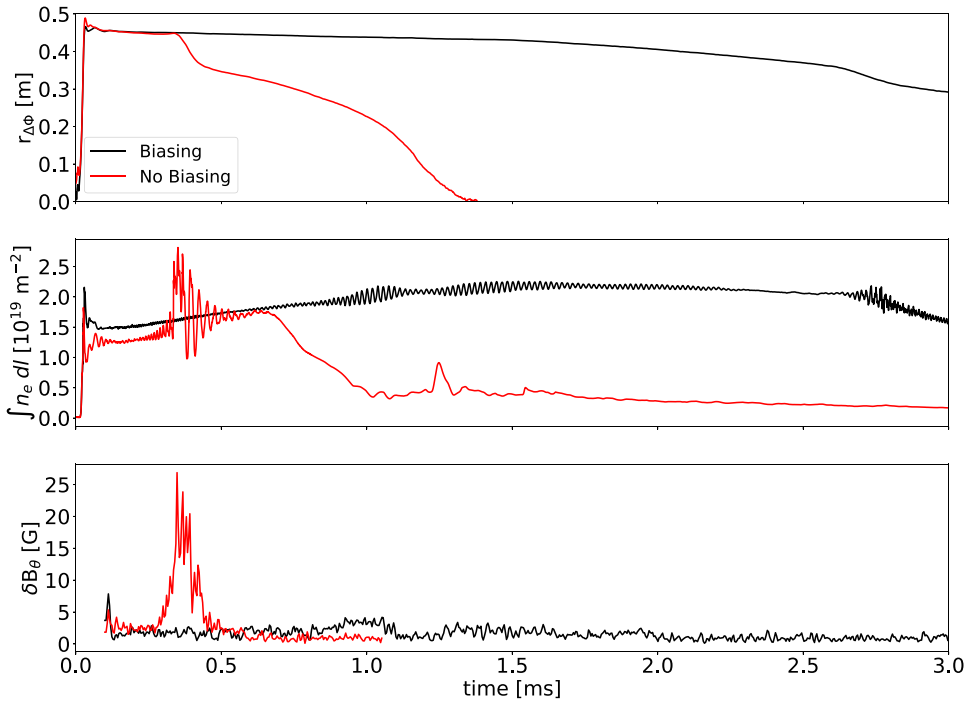

Figure 8. Effect of edge biasing on FRC plasma stability. From the top panel to the bottom: excluded-flux radius, line-integrated electron density from midplane FIR interferometer, and $n = 2$ mode amplitude estimated by SVD analysis using Mirnov probe array.

the case of no edge biasing a large amplitude of $n = 2$ MHD perturbation (elliptical distortion) appears and grows early in the discharge ($t < 0.5$ ms: signals on both line-integrated density and $n = 2$ mode amplitude) which leads to a loss of internal energy, particles, and ultimately to the FRC lifetime much shorter than that of $-E_r$ applied edge biasing case. The MHD perturbation amplitude is determined using singular value decomposition (SVD) analysis [44] of an azimuthal array of eight Mirnov probes located near the central region of the CV [28]. In the case without edge biasing the peak of the $n = 2$ mode amplitude correlates well with the time when the excluded-flux radius is abruptly dropped as shown in figure 8; while, with effective edge biasing FRC plasma is globally stabilized and no strong $n = 2$ mode activity is observed, thus extending plasma lifetime/duration. This edge biasing effect on FRC stability, together with NBI, is consistent with C-2/2U experiments [7, 9, 10].

As the second example of edge biasing scheme and its effect, an electrical potential of the central electrode inside outer divertors changed to be positive, meaning $+E_r$ applied, at which ion Doppler spectroscopy located near the midplane has indicated a clear edge biasing effect on plasma rotation and its velocity [45], as shown in figure 9. The instrument has a fan array of 15 viewing chords that covers about a half of the CV cross-section; an impact parameter of the outer-most viewing chord is ~0.39 m and the system measures oxygen $4+$ line emission at 278.1 nm. In a typical FRC without edge biasing, impurity ions start to rotate in the electron diamagnetic direction and then reverse the direction/rotation gradually into the ion diamagnetic direction as can be seen in figure 9(*a*); while, in the positively-biased edge control case (i.e. applying $+E_r$), impurity ions are accelerated to rotate in the ion diamagnetic direction thus reaching to the maximum velocity earlier in time as compared to non-biasing case. Note that an instrumental error of this ion rotation measurement is quite small, only a few km s^{-1}. Based on the impurity ion velocity distribution and its angular velocity, it is found that core region of the plasma exhibits a rigid-rotor profile with no velocity shear while the shear is observed near the edge inside the FRC separatrix. The peak velocity of the plasma rotation as well as shear flow can be controlled by edge-biasing systems as can be seen in figure 9(*b*), where the total biasing current is estimated from power supplies on both sides of the device. The more biasing current is driven/applied to open-field-line plasmas, the higher rotation velocity and shear flow can be obtained. However, it is also found that applying too high biasing current could cause/excite global MHD instabilities such as $n = 1$ wobble and $n = 2$ rotational modes, which is dependent on the applied radial electric field amplitude as well as its polarity. This FRC rotation and its velocity can be discussed using momentum equation, as equation (1) of [7].

Magnetic fields in both inner and outer divertors can also be varied by squeezing or flaring flux bundles to change the radial electric field (i.e. varying E_r/r), which is also important to generate the sufficient $E \times B$ shear flow for FRC stability control, and perhaps contributes to some auxiliary heating on SOL/open-field-line plasmas. In fact, it was observed in C-2U that flaring magnetic field at end divertor regions has produced ~20%–30% hotter core plasma temperatures of FRC's as compared to non-flaring case [5, 6]. Changing magnetic field configuration inside the inner divertors is the key to establishing a new operating regime that can provide more effective control on SOL/edge plasmas, much closer to the core FRC inside the CV as compared with that from outer divertors, as

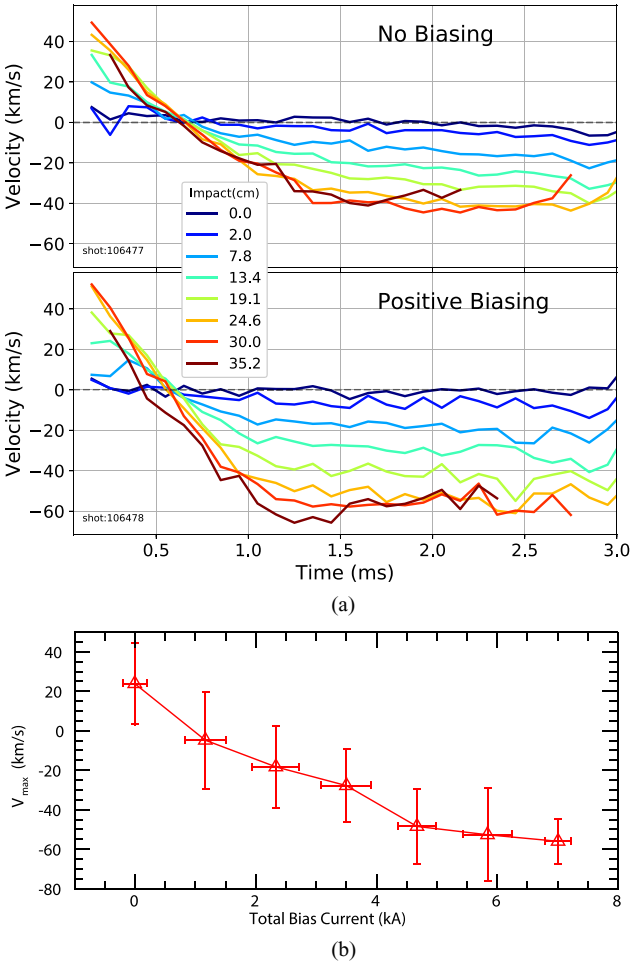

Figure 9. Plasma rotation and velocity measurement by ion Doppler spectroscopy: (*a*) rotation velocity evolution at various impact parameters of viewing chords in the cases with and without edge biasing, in which only a half of the chords are shown for simplicity and also error bars are not included because they are within a few km s^{-1} level; (*b*) peak rotation velocity at various edge-biasing operating conditions where total biasing current is estimated from biasing power supplies on both sides, and plots are averaged over several similar shots.

can be seen in figure 1(*c*). In the early C-2W experimental campaign the machine was operated as C-2U like configuration (in OP1.1), meaning no magnetic field flaring at inner divertor regions as shown in figure 1(*b*), to produce long-lived stable FRCs whose duration has to be long enough in order to adequately transfer edge biasing/control regions from outer to inner divertors. Note that magnetic field switching time (from straight field to flared field configurations by reversing a current direction in the fast-switching coils that typically starts at around $t \sim 0$ or slightly earlier) inside inner divertors is about a few milliseconds so that achieving FRC plasma duration of ~5 ms or longer in OP1.1 was one of our key early scientific milestones. In order to verify the inner-divertor magnetic field profile as well as its time evolution during the field flaring, a custom magnetic probe array was temporally installed and scanned around inside the inner divertor. It was found that the actual field measurements are relatively well matched with field calculations using an eddy-current finite element model (difference within ~10% in amplitude). With a full magnetic field expansion at inner divertor regions, we can achieve a mirror ratio of 30 or larger where the ratio is defined as the confinement mirror field B_{mirror} over the expanded inner-divertor field amplitude B_{expand} (i.e. $R_{\mathrm{mirror}} = B_{\mathrm{mirror}}/B_{\mathrm{expand}}$). While the inner divertor fields expand, the mirror ratio for FRC confinement inside the CV (i.e. $R_{\mathrm{m}} = B_{\mathrm{mirror}}/B_0$; B_0 is vacuum magnetic field at midplane) is maintained greater than 2.5 throughout the plasma discharge in order to not only assist initial FRC collisional-merging process but also control plasma axial position.

Figure 10 shows an example of two plasma discharges under different machine configurations in operation phases OP1.1 and OP1.2: C-2U-like machine configuration (no inner-divertor magnetic-field flaring) with negatively-biased edge control from outer divertors in OP1.1 (shot #104989), and flared inner-divertor field configuration with positively-biased edge control from outer divertors in OP1.2 (shot #107322). Note that NBs are injected for longer than FRC plasma lifetime in both cases. Time evolution of the electron temperature profiles, measured by midplane time-resolved multipoint Thomson scattering system [31], for those shots are also shown in figure 11, both of which exhibit a hollow radial profile as anticipated by the FRC structure. Under the C-2U-like machine configuration using only outer-divertor edge biasing/control, FRC plasma has successfully lived up to 8+ ms which is long enough to move on to the next operating phase (meaning that OP1.1 to OP1.2: edge biasing/control primarily from inner divertors with magnetic field flaring). In those long-lived FRC plasma discharges, a micro-burst type of weak/benign instability induced by injected fast ions has been observed [30], as previously seen in C-2U [46]. We have recently begun a new operating mode in OP1.2, in which extensive optimization processes have been executed both manually and with Google's optimization tool/algorithm [40] on many C-2W subsystems such as pulsed powers, magnets including fast-switching coils and formation DC coils, edge biasing/control systems and wall conditioning, which resulted in relatively good initial FRC plasma states with higher electron temperature as seen in figure 10 (shot #107322). In this inner-divertor operating mode with magnetic field flaring (OP1.2), FRC plasma duration is not quite as long as outer-divertor operating mode (OP1.1) because the transition of the edge/boundary control regions from outer to inner divertors is not yet adequately performed; this might be due to a lack of stabilization effect and increased parallel transport property by unfavorable open-field-line plasma conditions during the transition of edge control areas. However, this result of early experimental campaign in OP1.2, indicating high initial T_{e} state as well as increasing the temperature for a short period of time around $t \sim 1$–2 ms as can be seen in figures 10 and 11(*b*), is quite encouraging and promising result in this operation phase before NB input power is increased in operations phase 2.

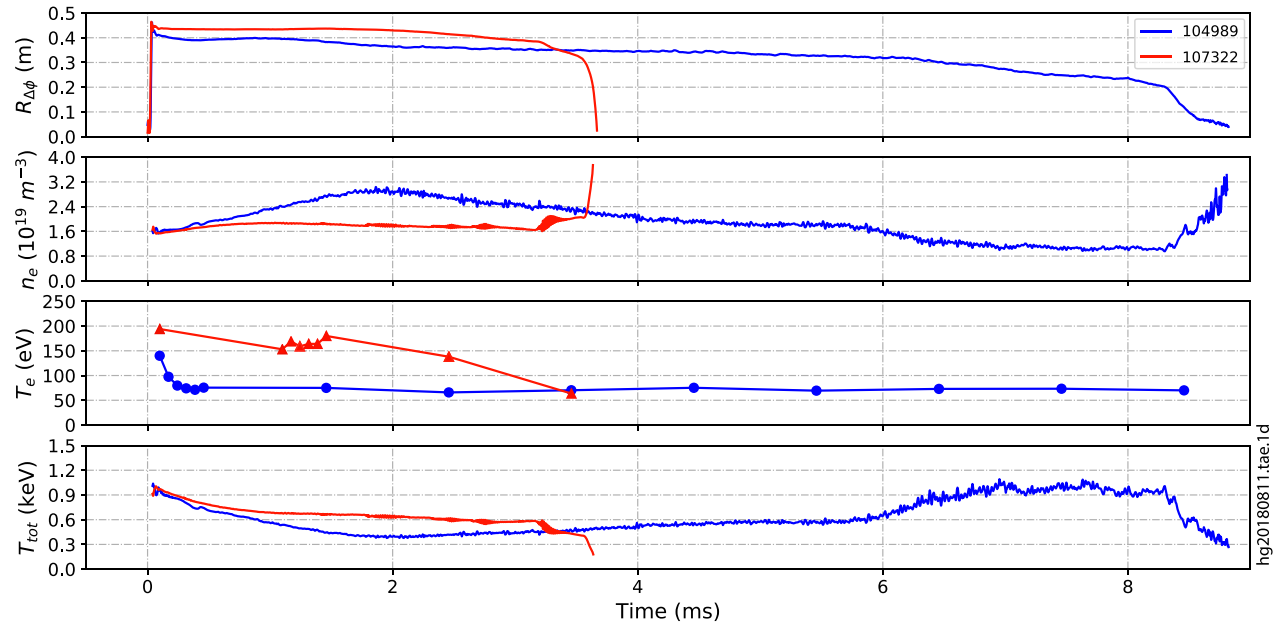

Figure 10. Examples of typical plasma discharges under different machine configurations: shot #104989 in OP1.1—without inner-divertor magnetic-field flaring and with outer-divertor edge biasing, C-2U like configuration; shot #107322 in OP1.2—with field flaring and outer-divertor biasing (positively). From the top panel to bottom: excluded-flux radius, electron density, electron temperature (averaged inside FRC separatrix), and total temperature estimated from pressure balance. Thomson scattering system can operate two modes together: (i) a 30-pulse chain at 1 kHz; and (ii) six pulses at 13 kHz or four pulses at 20 kHz burst with selectable start time of interest [31]. Note that NBs are injected for longer than FRC plasma lifetime in both discharges.

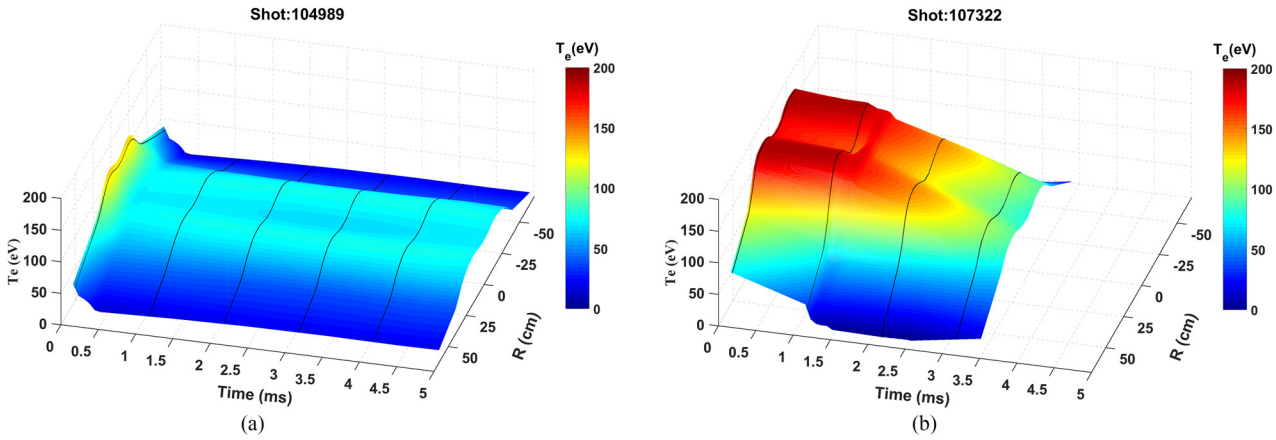

Figure 11. Time evolutions of electron temperature radial profile on (*a*) shot #104989 in OP1.1 (C-2U like configuration; edge biasing from outer divertors) and (*b*) shot #107322 in OP1.2 (with inner-divertor magnetic field flaring and outer-divertor edge biasing), measured by midplane Thomson scattering system. Note that low temperature regions (color in dark blue) are mostly outside of FRC separatrix.

4. Summary

The C-2W device was newly constructed with substantial subsystem upgrades from C-2U. C-2W initially demonstrated a robust FRC formation and translation through the newly installed inner divertor with adequate guide magnetic field, and then produced improved initial FRC plasma states after merging of the two colliding FRCs (relative speed of collision up to ~1000 km s^{-1}) as expected from the system upgrades. The merged initial FRC state exhibited higher plasma temperatures (T_e ~ 250 + eV, T_{tot} exceeding 1.5 keV) than C-2U. Under outer-divertor operating condition in OP1.1 (without flaring magnetic field at inner divertor regions) like C-2U configuration, stable and long-lived FRC plasma state was obtained by effective edge biasing and NBI; FRC achieved ~9 ms plasma lifetime which is equivalent to C-2U performance. Under inner-divertor operating condition with magnetic field flaring in OP1.2, electron temperature inside FRC appeared to stay hot and increase for a short period of time. The C-2W NB system is being further upgraded to be able to ramp up beam injection energy, at which the total injection power will go up to ~21 MW and then FRC plasma pressure is expected to ramp up as well in the next operation phase (OP2).

Acknowledgments

The authors wish to thank the entire TAE Team for their dedicated work and effort on the C-2W project, our Budker Institute colleagues for many key contributions to our experiments including studies of open-field-line plasmas and divertor physics as well as the key neutral beam development, other scientific and engineering collaborators including Google team for system/plasma optimization as well as plasma reconstruction effort, and our shareholders who made this exciting research effort possible.

ORCID iDs

H. Gota https://orcid.org/0000-0001-6475-2912
M.W. Binderbauer https://orcid.org/0000-0002-2698-4744
B.H. Deng https://orcid.org/0000-0002-7025-2970
S.A. Dettrick https://orcid.org/0000-0002-1756-4625
D.K. Gupta https://orcid.org/0000-0003-4849-1198
R.M. Magee https://orcid.org/0000-0001-6697-7891
T. Roche https://orcid.org/0000-0003-0840-4731
J.A. Romero https://orcid.org/0000-0001-7585-1350
L.C. Steinhauer https://orcid.org/0000-0003-2227-7345
M.C. Thompson https://orcid.org/0000-0002-5907-742X
E. Trask https://orcid.org/0000-0003-4984-6579
K. Zhai https://orcid.org/0000-0002-8432-3696
M. Beall https://orcid.org/0000-0002-5070-6824
N.G. Bolte https://orcid.org/0000-0002-3702-4650
A.M. DuBois https://orcid.org/0000-0003-0947-8038
E.M. Granstedt https://orcid.org/0000-0002-7691-4883
C.K. Lau https://orcid.org/0000-0001-6702-1461
M. Nations https://orcid.org/0000-0002-7795-1555
A. Ottaviano https://orcid.org/0000-0003-0255-3824
T.M. Schindler https://orcid.org/0000-0002-6856-1707
D. Sheftman https://orcid.org/0000-0002-7856-9032
R.J. Smith https://orcid.org/0000-0002-3595-781X
T. Asai https://orcid.org/0000-0001-9440-0117
J.C. Platt https://orcid.org/0000-0002-5652-5303

References

[1] Tuszewski M. 1988 Field reversed configurations *Nucl. Fusion* **28** 2033
[2] Steinhauer L.C. 2011 Review of field-reversed configurations *Phys. Plasmas* **18** 070501
[3] Binderbauer M.W. *et al* 2010 Dynamic formation of a hot field reversed configuration with improved confinement by supersonic merging of two colliding high-β compact toroids *Phys. Rev. Lett.* **105** 045003
[4] Binderbauer M.W. *et al* 2015 A high performance field-reversed configuration *Phys. Plasmas* **22** 056110
[5] Binderbauer M.W. *et al* 2016 Recent breakthroughs on C-2U: Norman's legacy *AIP Conf. Proc.* **1721** 030003
[6] Gota H. *et al* 2017 Achievement of field-reversed configuration plasma sustainment via 10 MW neutral-beam injection on the C-2U device *Nucl. Fusion* **57** 116021
[7] Tuszewski M. *et al* 2012 Field reversed configuration confinement enhancement through edge biasing and neutral beam injection *Phys. Rev. Lett.* **108** 255008
[8] Gota H. *et al* 2015 Improved confinement of C-2 field-reversed configuration plasmas *Fusion Sci. Technol.* **68** 44
[9] Guo H.Y. *et al* 2015 Achieving a long-lived high-beta plasma state by energetic beam injection *Nat. Commun.* **6** 6897
[10] Schmitz L. *et al* 2016 Suppressed ion-scale turbulence in a hot high-β plasma *Nat. Commun.* **7** 13860
[11] Rosenbluth M.N. *et al* 1962 Finite Larmor radius stabilization of 'weakly' unstable confined plasmas *Nucl. Fusion Suppl.* **1** 143
[12] Fulton D.P. *et al* 2016 Gyrokinetic simulation of driftwave instability in field-reversed configuration *Phys. Plasmas* **23** 056111
[13] Onofri M. *et al* 2015 Simulations of the C-2/C-2U field reversed configurations with the Q2D code *Bull. Am. Phys. Soc.* **60** BP12.00032
[14] Beall M. *et al* 2016 Improved density profile measurements in the C-2U advanced beam-driven field-reversed configuration (FRC) plasmas *Rev. Sci. Instrum.* **87** 11E128
[15] Rej D.J. and Tuszewski M. 1984 A zero-dimensional transport model for field-reversed configurations *Phys. Fluids* **27** 1514
[16] Trask E. *et al* 2016 C-2U experimental transport analysis *Bull. Am. Phys. Soc.* **61** CP10.00064
[17] Kaye S.M. *et al* 2007 Confinement and local transport in the National Spherical Torus Experiment (NSTX) *Nucl. Fusion* **47** 499
[18] Kaye S.M. *et al* 2013 The dependence of H-mode energy confinement and transport on collisionality in NSTX *Nucl. Fusion* **53** 063005
[19] Valovic M. *et al* 2009 Scaling of H-mode energy confinement with I_p and B_t in the MAST spherical tokamak *Nucl. Fusion* **49** 075016
[20] Galeotti L. *et al* 2011 Plasma equilibria with multiple ion species: equations and algorithm *Phys. Plasmas* **18** 082509
[21] Ivanov A.A. and Prikhodko V.V. 2013 Gas-dynamic trap: an overview of the concept and experimental results *Plasma Phys. Control. Fusion* **55** 063001
[22] Bagryansky P.A. *et al* 2016 Recent progress of plasma confinement and heating studies in the gas dynamic trap *AIP Conf. Proc.* **1771** 020003
[23] Guo H.Y. *et al* 2011 Formation of a long-lived hot field reversed configuration by dynamically merging two colliding high-b compact toroids *Phys. Plasmas* **18** 056110
[24] Matsumoto T. *et al* 2016 Development of a magnetized coaxial plasma gun for compact toroid injection into the C-2 field-reversed configuration device *Rev. Sci. Instrum.* **87** 053512
[25] Asai T. *et al* 2017 Compact toroid injection fueling in a large field-reversed configuration *Nucl. Fusion* **57** 076018
[26] Vinyer I.V. 2014 A 12-barrel deuterium pellet injector for the C-2 field-reversed configuration device *Instrum. Exp. Tech.* **57** 508
[27] Thompson M.C. *et al* 2016 Diagnostic suite of the C-2U advanced beam-driven field-reversed configuration plasma experiment *Rev. Sci. Instrum.* **87** 11D435
[28] Roche T. *et al* 2018 Magnetic diagnostic suite of the C-2W field-reversed configuration experiment *Rev. Sci. Instrum.* **89** 10J107
[29] Dubois A.M. *et al* 2018 Design of a custom insertable probe platform for measurements of C-2W inner divertor plasma parameters *Rev. Sci. Instrum.* **89** 10J115
[30] Deng B.H. *et al* 2018 Development of a three-wave far-infrared laser interferometry and polarimetry diagnostics for the C-2W FRC experiment *Rev. Sci. Instrum.* **89** 10B109
[31] Zhai K. *et al* 2018 Thomson scattering systems on C-2W field-reversed configuration plasma experiment *Rev. Sci. Instrum.* **89** 10C118

[32] Schmitz L. *et al* 2018 Combination doppler backscattering/ cross-polarization scattering diagnostic for the C-2W field-reversed configuration *Rev. Sci. Instrum.* **89** 10H116
[33] Griswold M.E. *et al* 2018 Particle and heat flux diagnostics on the C-2W divertor electrodes *Rev. Sci. Instrum.* **89** 10J110
[34] Titus J.B. *et al* 2018 Secondary electron emission detectors for neutral beam characterization on C-2W *Rev. Sci. Instrum.* **89** 10I123
[35] Granstedt E.M. *et al* 2018 Calibration and applications of visible imaging cameras on the C-2U advanced beam-driven field-reversed configuration device *Rev. Sci. Instrum.* **89** 10E103
[36] Romero J.A. *et al* 2018 Inference of field reversed configuration topology and dynamics during Alfvenic transients *Nat. Commun.* **9** 691
[37] Thompson M.C. *et al* 2018 Integrated diagnostic and data analysis system of the C-2W advanced beam-driven field-reversed configuration plasma experiment *Rev. Sci. Instrum.* **89** 10K114
[38] Mok Y. *et al* 2010 Modeling of dynamic FRC formation *Bull. Am. Phys. Soc.* **55** GP9.00097
[39] Trask E. *et al* 2018 Formation and translation experiments on the C-2W experiment *Bull. Am. Phys. Soc.* **63** PP11.00080
[40] Baltz E.A. *et al* 2017 Achievement of sustained net plasma heating in a fusion experiment with the optometrist algorithm *Sci. Rep.* **7** 6425
[41] Ono Y. *et al* 1996 Ion acceleration and direct ion heating in three-component magnetic reconnection *Phys. Rev. Lett.* **76** 3328
[42] Yamada M. 2016 Formation and sustainment of field reversed configuration (FRC) plasmas by spheromak merging and neutral beam injection *AIP Conf. Proc.* **1721** 020005
[43] Gota H. *et al* 2018 Overview of C-2W field-reversed configuration experimental program *Bull. Am. Phys. Soc.* **63** PP11.00078
[44] Nardone C. 1992 Multichannel fluctuation data analysis by the singular value decomposition method. Application to MHD modes in JET *Plasma Phys. Control. Fusion* **34** 1447
[45] Beall M. *et al* 2018 Correlations between impurity ion tangential velocities and electron density rotational modes in the C-2W experiment *Bull. Am. Phys. Soc.* **63** PP11.00091
[46] Deng B.H. *et al* 2018 A new fast ion driven micro-burst instability in a field reversed configuration plasma *Nucl. Fusion* **58** 126026